J. Astron. Space Sci., Vol.7, No.2, 73-103(1990)

CORRELATION AMONG MORPHOLOGICAL CLASSIFICATIONS AND MASS TO LUMINOSITY(M/L) RATIOS OF EXTRA GALAXIES

Mun-Suk Chun and Kyung-Sun Na
Department of Astronomy & Atmospheric Science
Yonsei University
(Received November 11, 1990 ; Accepted November 30, 1990)

Abstract

Morphological luminosity parameters(μ_e, r_e, μ_o, α^{-1}) and D/B were estimated from the decomposition of surface brightness distributions of 28 extra galaxies. Decomposition was made using the standard non-linear least square fitting method and we used the seeing convolved model to get the central brightness of these galaxies. Masses and M/L_B were calculated using rotational velocities of these galaxies from the fitting to the generalized Toomre's mass model.

I. Introduction

After the morphological classification of extra galaxies by Hubble(1936), many attempts were made to classify extra galaxies quantitatively(Sandage 1975). However rapid developement of the recent observational techniques like the CCD observation makes it possible to classify extra galaxies qualitatively. As the basic structural parameters of extra galaxies will reflect the formation and evolution of these objects, it is meaningful to study dynamical parameters of the disk and spheroidal components of these galaxies. Unlike the H-R diagram in stars, there are no such simple diagrams to explain physically for the formation. structure and evolution of galaxies. Therefore we want to find any correlation among the morphological classification, structural, physical and dynamical parameters of galaxies. In this paper we calculated physical and dynamical parameters using the surface brightness distributions and rotational velocities of 28 extra galaxies in the range of Sa to Sc morphological type.

The surface brightness distributions of extra galaxies made it possible to divide galaxies as 2 systems: the bulge component where the surface brightness distribution fitted to $r^{1/4}$ law(de Vaucouleurs 1953) and the disk component which is well fitted to the exponential distribution law(Freeman 1970). However there exists many galaxies in where surface brightness distributions are not fitted well to the empirical law(Okamura 1988). This dispersion was interpreted as the result of recent star formations(Talbolt *et al.* 1979), or the existence of the bar structure and the accompanied galaxies(Boronson 1981).

Many attempts were made to separate the spheroidal and disk components through the decomposition process(Kormendy 1977;King 1978;Burstein 1979;Boronson 1981;Kent 1985). From this decomposition, they can estimate parameters of each component and the disk to bulge ratios of galaxies.

Kormendy(1977) suggested two methods to make the decomposition as like the iterrative fitting method and the standard non-linear least square method. In the central regions of extra galaxies, seeing effect becomes serious(King 1978). This seeing effect can be corrected through the convolved method(Schweizer 1979, 1981, Schombert and Bothun 1987, Simien and de Vaucouleurs 1986).

In the case of the same Hubble type rotation velocity of the brighter galaxy tends to be ~100 km/sec faster than the fainter one, and the maximum rotation velocity becomes slower from Sa to Sc(Rubin *et al.* 1980, 1985). Masses of disk galaxies can be calculated from the observed rotation curves(Mestel 1963; Toomre 1963; Brandt 1960). From this mass we can estimate the mass to luminosity(M/L) ratio, and this M/L value will give some information concerning the existence of the dark matter in galaxies.

II. Surface Brightness Distribution

Basic characters of the used 28 extra galaxies are listed in Table 1. We used the published surface luminosity distributions and rotation velocities of these 28 galaxies. The used Hubble constant is 75km sec^{-1} Mpc^{-1} and the luminosity data are converted to B magnitute system.

The r-band observed data by Kent(1984, 1986, 1988) were converted to B-magnitude system as

$$B = r + 0.10 + 1.18(B - V)$$

The g-band data by Jarvis(1988) were converted to $r = g - (g - r)$, and then these data were converted to B system as above.

The correction to the seeing effect, we used the full width at half maximum(FWHM) which comes from the observed star image in plates. The used FWHM values are listed in Table 1.

Table 1. Basic characters of 28 galaxies

NAME (1)	class (2)	T (3)	l(°) (4)	b(°) (5)	AC (6)	Y (7)	D(Mpc) (8)	ε (9)	FWHM(") (10)	i(°) (11)	V_h(km/sec) (12)	Source (13)	(14)
N701	Sc(s) II, 2;	5	164.67	−67.6			24.7	0.68	3.3	67	1795	2	1
N753	Sc(rs) I	4	137.71	−25.05	9	f	68	0.33	2.6	46	4895	2	1
N1085	SAb(a)	3	169.46	−48.6	3		90 7	0.35	2.6	42	6784	2	2
N1087	Sc(s) III, 3	5	173.77	−51.65	2	a	20.5	0.36	2.1	63	1503	1	1
N1357	Sa(s)	1	201.55	−49.97	12		26.2	0.22	2.6	54	2038	3	3
N1543	RSBD$_{2/3}$(o)/a	−2	268.4	−44.53			13.4	0.45	2.5	65	1130	4	4
N1574	SBO$_2$	−2	266.88	−42.58			13.4	0.05	2.5	31	1009	4	4
N1620	SATbc(a)	4	196.16	−29.67			45.6	0.68	4.3	72	3490	2	2
N2639	Sa	1	168.88	38.19			44.3	0.60	2.3	53	3193	1	3
N2708	SASb:(a)	3	231.55	25.67			23.7	0.60	3.0	67	1985	2	2
N2775	Sa(r)	2	223.26	34	3	gk	16.2	0.21	2.3	39	1355	3	3
N2815	Sb(s) I−II	3	252.18	17.4			30.3	0.70	3.1	77	2542	2	2
N2844	Sa(r)	1	182.11	45.15			19.9	0.50	2.5	64	1498	3	3
N3054	SBbc(s) I	3	260.18	22.15	9		28.7	0.44	3.1	55	2425	2	2
N3593	Sa pec	0	240.44	63.21		g	8.3	0.62	3.4	69	637	3	3
N3898	Sa I	2	139.76	58.97	3	k	15.4	0.41	3.1	46	1165	3	3
N4378	Sa(s)	1	286.08	66.93	6	gk	32.4	0.22	3.4	23	2544	3	3
N4448	Sb(r) I−II	2	195.3	84.67		g	12.7	0.65	3.0	71	657	2	2
N4477	SBO$_{1/2}$/SBa	−2	281.54	75.61			16.8	0.16	2.74	26	1306	5	4
N4682	Sc(s) II, 4	5	301.24	52.8	2		28.9	0.5	3.5	59	2307	2	1
N4698	Sa	2	300.61	71.35	3	k	13.3	0.61	2.8	68	1014	3	3
N4754	SBO,	−2	303.72	74.18			16.8	0.47	3.0	63	1307	4	4
N4800	Sb(rs) II−III	3	121.3	70.59			13	0.3	2.3	47	891	2	2
N6314	SaS I (RC2)	1	44.89	31.45			92	0.46	3 0	64	6642	3	3
N7171	Sb(r) I	3	43 44	−47.92	5		38.3	0.56	3.3	62	2727	2	2
N7217	Sb(r) II−III	2	86.5	−19.7	3	gk	16.5	0.1	2.9	32	955	2	2
N7537	SBTb(a)	4	82.76	−50.65			38.2	0.72	2 9	81	2675	2	2
N7606	Sb(r) I	3	69.09	−61.29		fg	31.7	0.59	3 3	74	2237	2	2

(2) RSA (Sandage and Tammann 1981) Classification
(3) RC2 (de Vaucouleurs, de Vaucouleurs and Corwin 1976) Classification
(4) longitude
(5) latitude
(6) Arm classification (Elmergreen and Elmergreen 1987)
(7) Yerkes classification (RC2)
(8) Distance (H=75km sec^{-1} Mpc^{-1} used)
(9) Ellipticity
(10) Full width at half maximum
(11) inclination
(12) Heliocentric velocity
(13) Surface brightness distribution
1. Kent. 1984 2. Kent, 1986
3. Kent, 1988 4. Jarvis *et al.* (1988)
5. Michard, 1985
(14) Rotation velocity
1. Rubin *et al.* (1980) 2. Rubin *et al* (1982)
3. Rubin *et al.* (1985) 4. Javis *et al.* (1988)

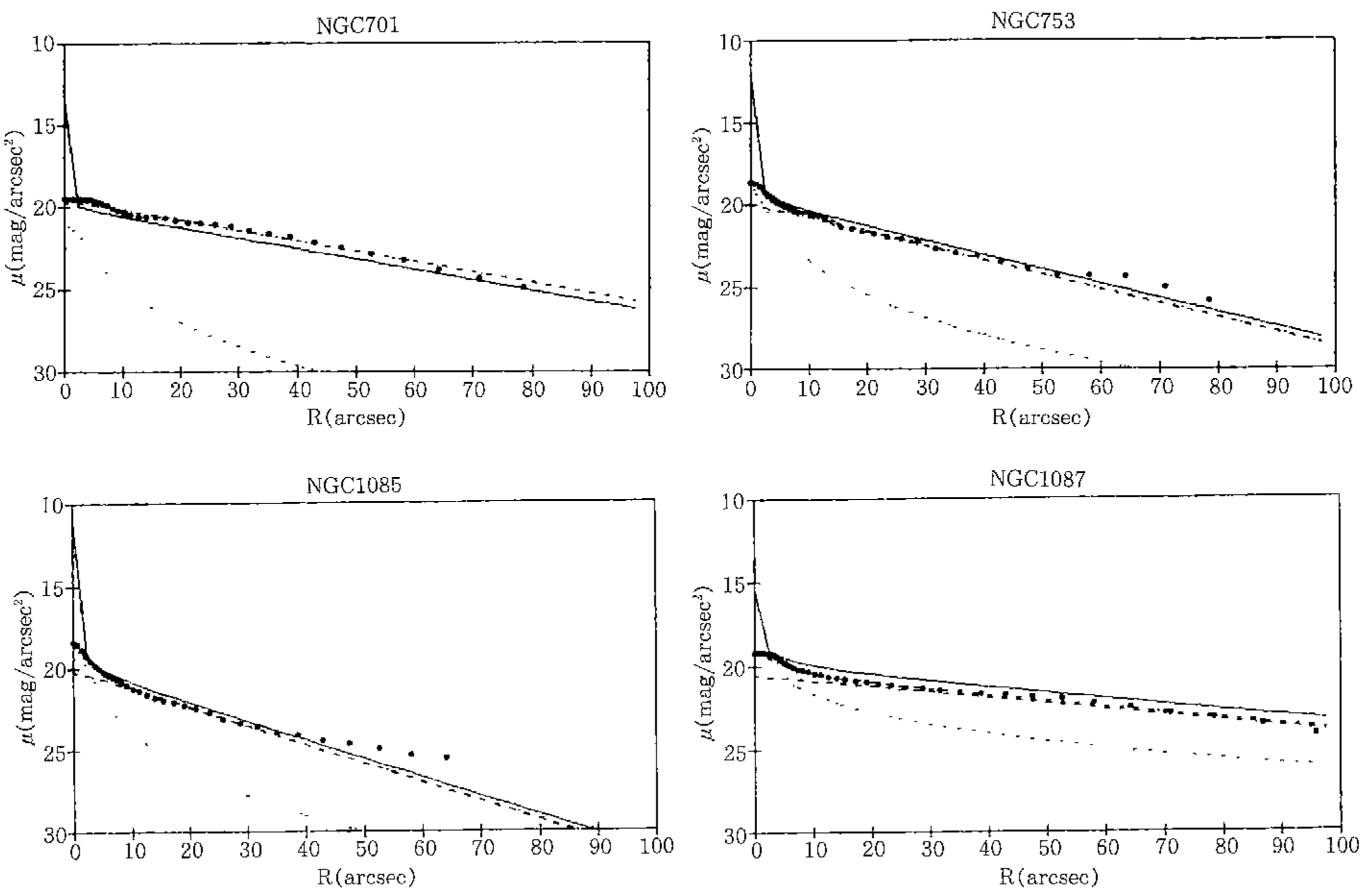

Fig. 1. Surface brightness distributions of 28 galaxies. All the observed luminosity profiles were divided into the spheroidal and disk component through the decomposition process. Filled circles are the observed brightness, straight lines indicate the unconvolued luminosity profiles. Dot means the spheroidal component and dashed line is the disk component. The mixture of dot and dashed line mean the convolved surface brightness distribution.

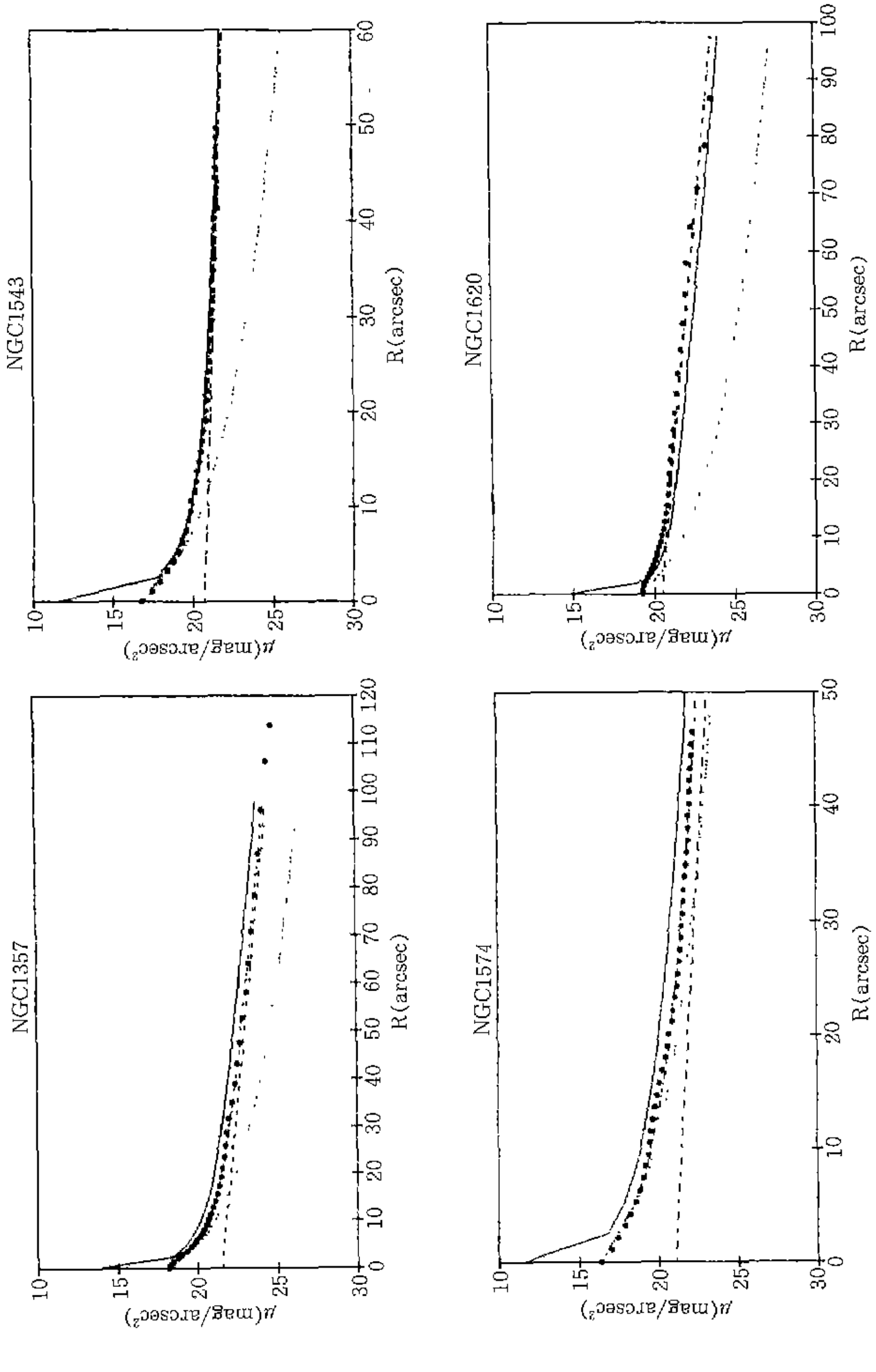

Fig. 1. Continued.

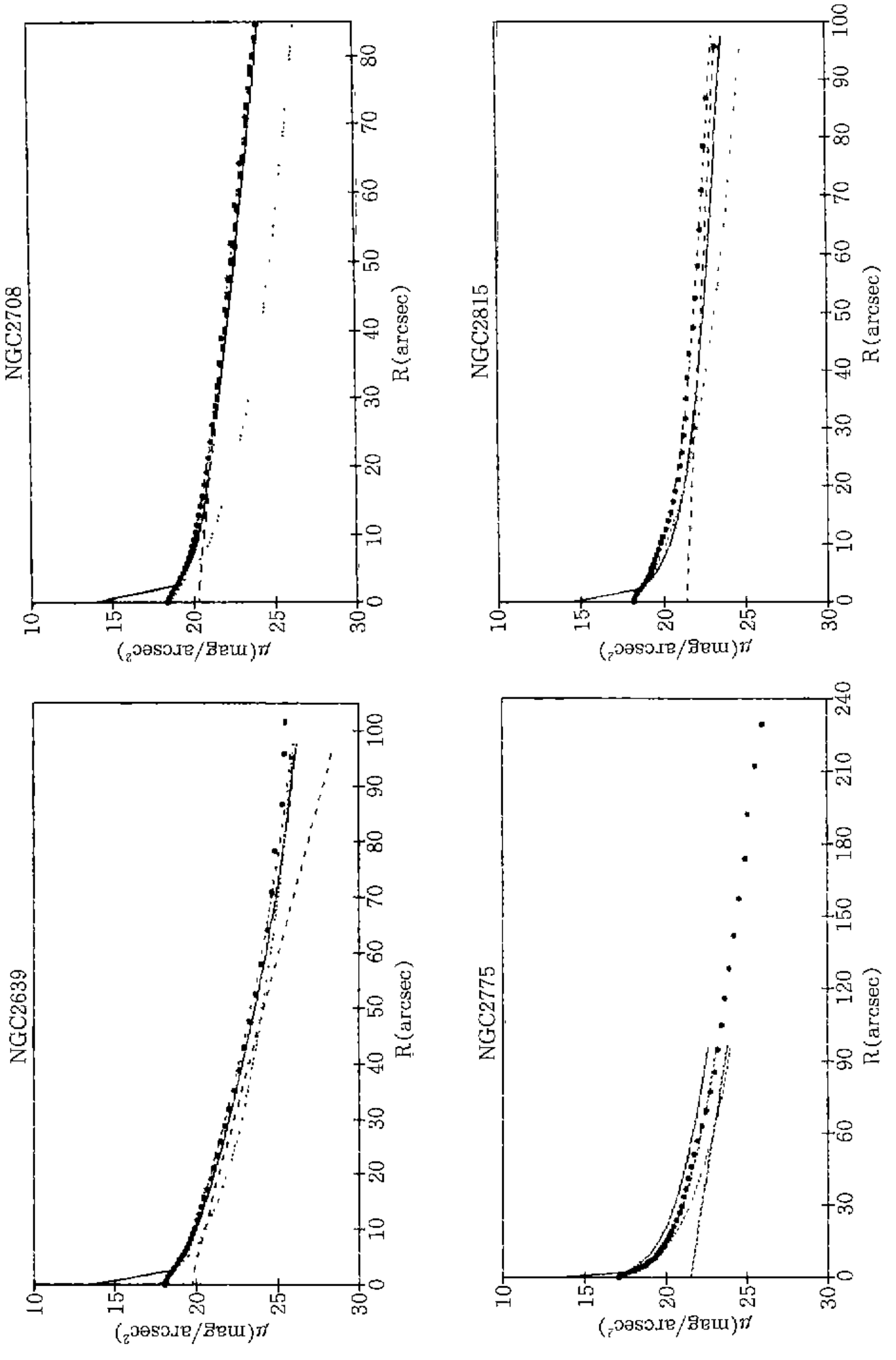

Fig. 1. Continued.

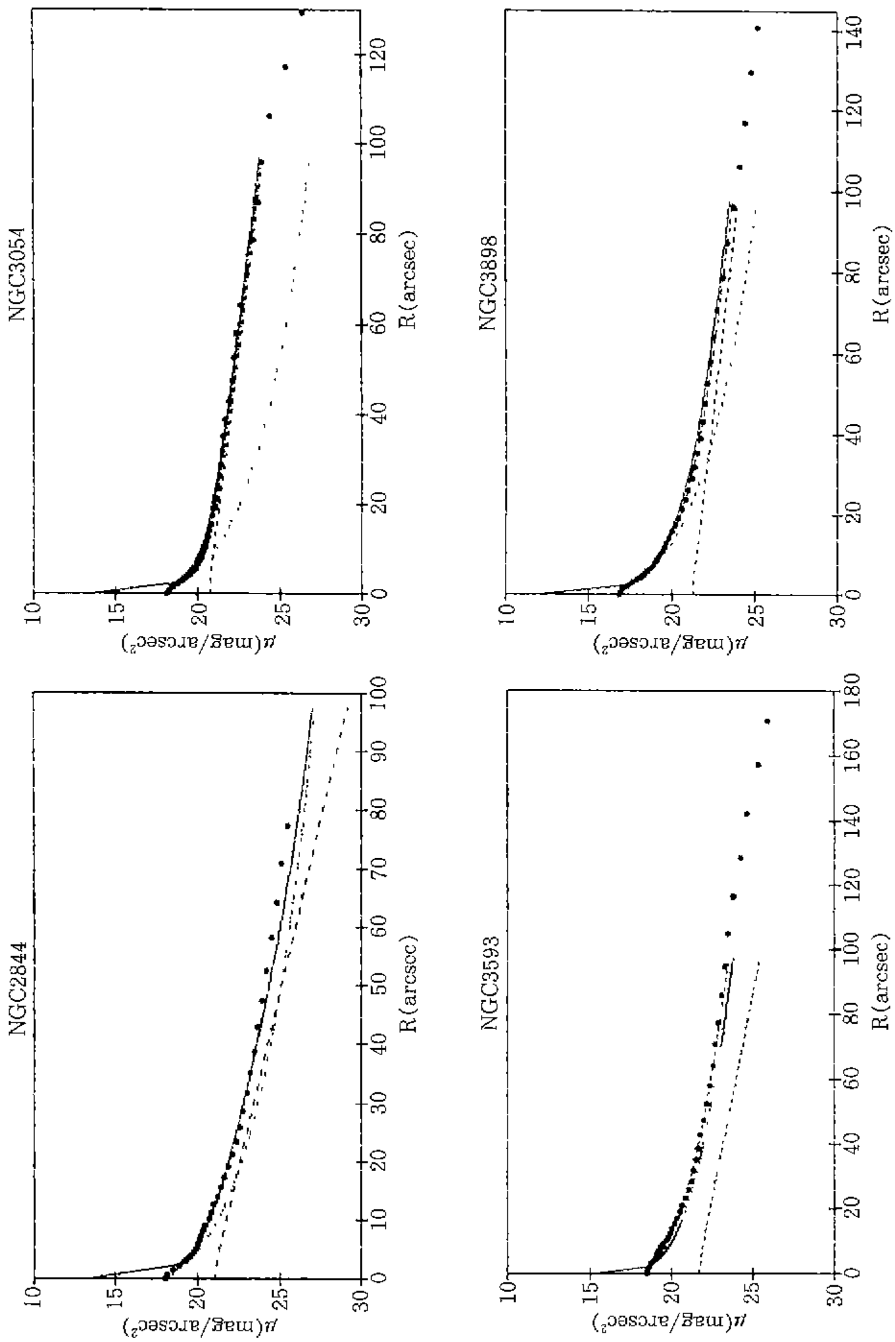

Fig. 1. Continued.

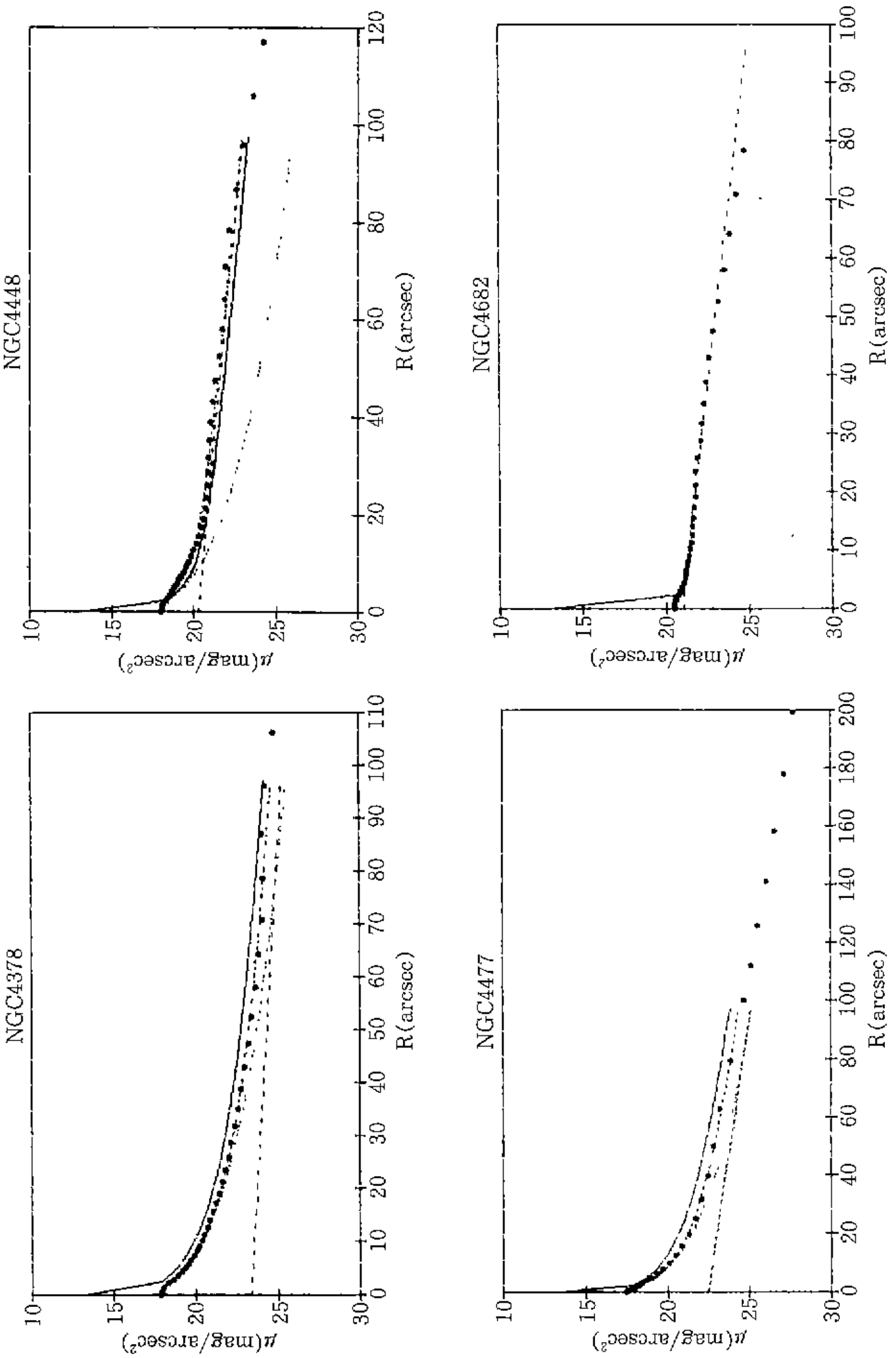

Fig. 1. Continued.

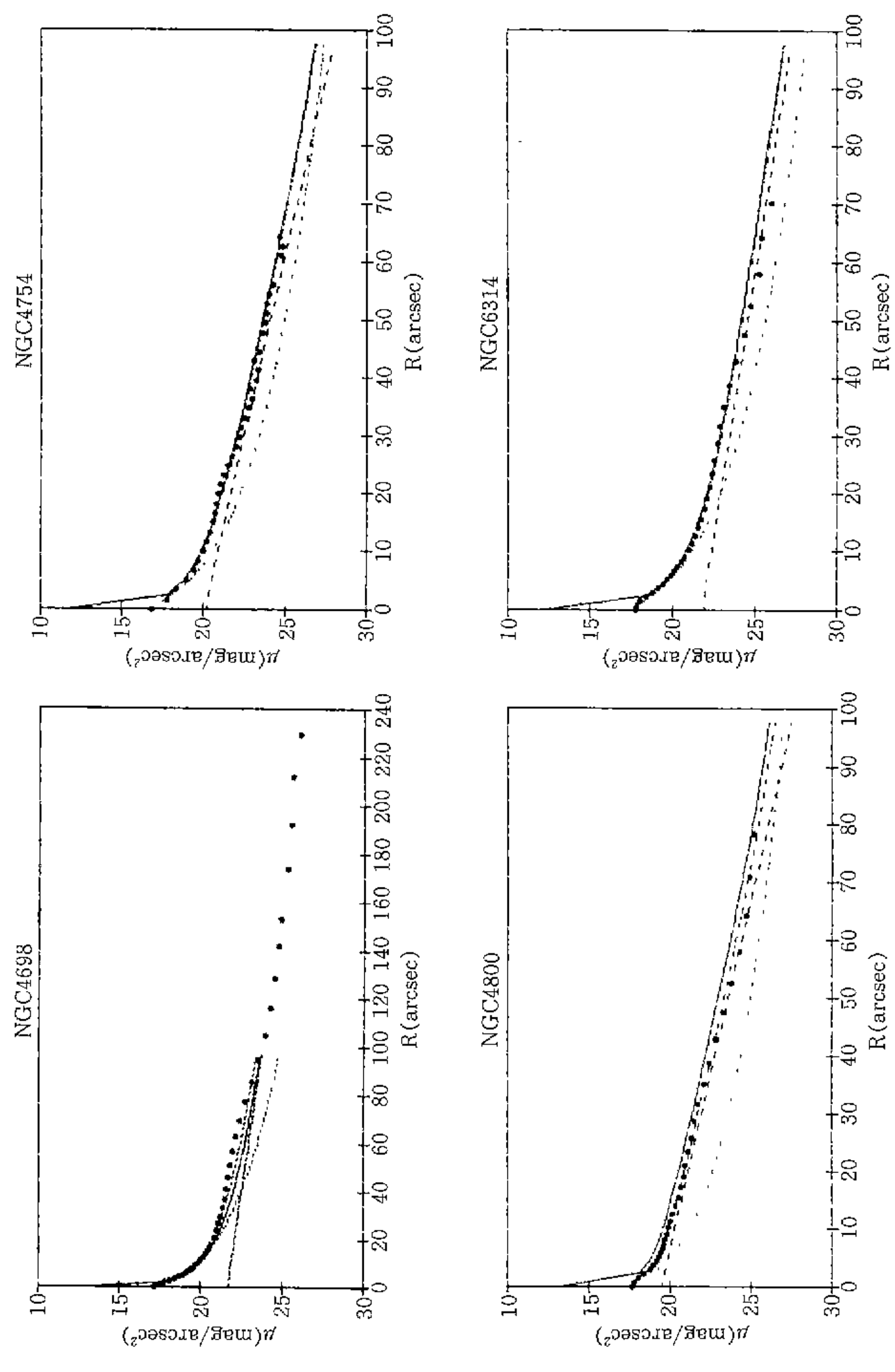

Fig. 1. Continued.

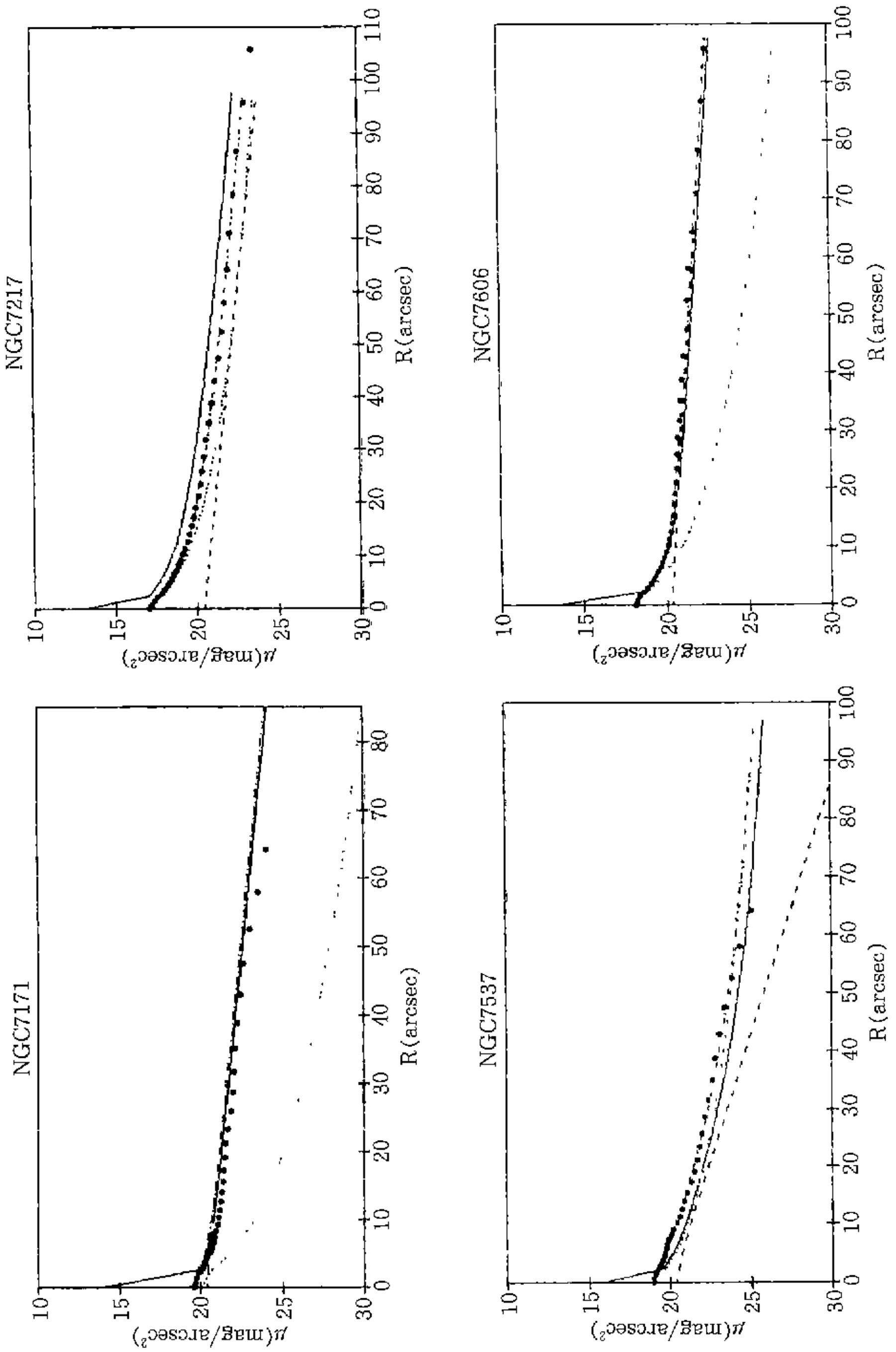

Fig. 1. Continued.

Using the surface brightness distribuations, we can calculate μ_e, r_e, μ_0 and α^{-1} and all these values of 28 extra galaxies are listed in Table 2. From these parameters we can get total luminosities(L_T) of 28 galaxies, luminosity of the spheroidal component(L_{bulge}), luminosity of the disk component(L_{disk}) and the disk to bulge ratio(D/B). Table 2 listed all these calculated values.

Table 2. Calculated physical parameters from the decomposition of the surface brightness distribution

NAME	μ_e (mag/□")	r_e (arcsec)	μ_0 (mag/□")	α^{-1} (arcsec)	D/B	L_B ($10^{10}M_\odot$)	L_D ($10^{10}M_\odot$)	L_T ($10^{10}M_\odot$)
N701	21.79	2.52	19.94	16.94	69.50	0.03	1.8	1.8
N753	20.51	3.36	19.56	12.37	9.13	1.2	11.0	12.0
N1085	19.36	1.97	19.78	9.43	4.33	2.1	8.9	11.0
N1087	23.76	43.78	20.03	31.28	4.45	0.9	3.9	4.8
N1357	22.01	20.79	21.02	35.94	2.08	1.7	3.4	5.1
N1543	19.81	7.48	20.54	49.44	6.27	0.4	2.6	3.0
N1574	19.84	14.64	20.32	24.80	0.51	1.6	0.8	2.4
N1620	22.99	15.76	20.83	31.51	8.24	1.2	9.4	11.0
N2639	21.94	18.27	19.80	11.84	0.84	3.8	3.1	6.9
N2708	22.19	15.39	20.39	23.10	3.31	0.64	2.1	2.7
N2775	22.79	45.40	21.00	46.00	0.60	3.7	2.2	5.9
N2815	22.71	31.60	21.90	53.36	1.69	2.7	4.5	7.2
N2844	21.77	13.09	20.88	12.80	0.61	0.5	0.3	0.8
N3054	21.84	15.12	20.52	31.21	4.02	1.2	4.9	6.1
N3593	23.67	84.28	21.85	27.48	0.16	0.06	0.09	0.7
N3898	20.35	16.76	21.06	38.15	0.75	0.7	0.5	1.3
N4378	21.51	23.45	22.88	55.07	0.43	5.3	2.3	7.6
N4448	21.80	16.87	20.62	38.57	4.31	0.3	1.3	1.6
N4477	21.75	30.52	21.85	39.29	0.42	1.9	0.8	2.7
N4682	21.33	1.33	20.90	26.05	160.90	0.02	2.4	2.4
N4698	21.71	25.18	21.91	50.62	0.94	0.08	0.8	1.6
N4754	19.96	7.75	19.99	13.36	0.81	0.06	0.05	1.1
N4800	21.60	14.80	19.08	13.20	2.26	0.3	0.7	1.0
N6314	20.45	7.39	21.71	19.56	0.62	10.5	6.4	17.0
N7171	22.27	6.02	20.84	24.88	17.97	0.2	4.0	4.2
N7217	21.39	47.11	19.76	30.22	0.52	5.9	3.1	9.0
N7537	24.23	46.55	20.63	9.37	0.31	2.2	0.7	2.9
N7606	21.22	9.42	20.38	42.84	12.48	1.0	13.0	14.0

In Figure 1 we plotted surface brightness distributions of 28 galaxies. Filled circles in Figure 1 denote the observed surface brightness and the straight line is the non-convolved brightness distribution. Dotted line indicates the spheroidal brightness distribution and the dashed line is the disk brightness distribution. The mixed dashed and dotted line is the convolved brightness distribution.

Ⅲ. Spheroidal and Disk Separation through Decomposition

Kormendy(1977) and Burstein(1979) used the decomposition process to divide the spheroidal and disk components from the luminosity distributions in galaxies. Decomposition can be done through the iterative fitting method or the standard non-linear least square method.

In the central region of a galaxy, correction should be made to ease the seeing effect. The apparent luminosity distribution $i(x, y)$, which is the seeing convolved, can be expressed as

$$i(x, y) = \int_{-\infty}^{+\infty} \int_{-\infty}^{+\infty} I(\zeta, \eta)\ S(x-\zeta, y-\eta)\ d\zeta d\eta$$

where $I(\zeta, \eta)$ is the luminosity distribution where the seeing is not convolved. The point spread function $S(x-\zeta, y-\eta)$ is the declined function of luminosity as a result of seeing effect. In the central region this function is Gaussian, while it becomes the exponentially declined luminosity function in the outer region.

Decomposition was made using the standard non-linear least square method, which comes from the minimum value of χ^2 from the repeated fitting to the obvserved luminosity distribution of a galaxy. χ^2 was defined by Schombert and Bothun(1987) as

$$\chi^2 = \frac{1}{\nu} \Sigma \frac{(\mu_i - \mu_{fit})^2}{\sigma^2}$$

where μ_i is the observed luminosity distribution and μ_{fit} is the calculated luminosity distribution of a galaxy. ν is the free parameter while σ indicates the standard deviation.

From the decomposition we can calculate morphological parameters like μ_e, r_e, μ_o, and α^{-1}.

The total luminosity of the spherical component can be estimated as

$$L_{bulge} = \int_0^{\infty} I_D(r)\ 2\pi r dr = 7.22\pi\ r_e^2 \mu_e$$

by Simien and deVaucouleurs(1986).

Freeman(1970) suggested the total luminosity of the disk component as

$$L_{disk} = \int_0^\infty I_D(r)\ 2\pi r dr = 2\pi\ \mu_o/\alpha^2$$

From the above equations we can calculate the D/B as

$$D/B = 0.28 \left(\frac{\alpha^{-1}}{r_e} \right) \frac{\mu_o}{\mu_e}$$

All these calculated parameters are listed in Table 2.

Ⅳ. *Rotation Curve Fitting and Mass Calculation*

Rotation curves of 28 galaxies were made from the spectroscopic data of Rubin(1980, 1982, 1985) and Javis *et al.*(1988). Maximum rotation velocity(V_{max}) and the radius to that velocity (r_{max}) were estimated from the polynomial fitting to the observed rotation curves. Masses of 28 galaxies were then calculated using the generalized Toomre's mass model(Lee 1988). The mass of a galaxy can be estimated from the 3 parameters(n, a_n, b_n), where a_n is the shape parameter of the rotation curve, and a_n and b_n can be estimated from the v_{max} and R_{max}. Observed rotation curves were fitted to model curves in Figure 2. Dots indicate the observed rotation velocities and dashed lines are model curves. Rotation curves of most sample galaxies tend to be flat or steady increase to the radial distance. So we used n=1 for all galaxies except NGC 4378 and NGC 7171, where we used n=2, About half of the sample galaxies we can fit well for whole galaxy with one structural parameter. However the other half we have to use two n values to fit to the spherical and disk components.

The calculated spheroidal, disk and total masses of galaxies are listed in Table 3.

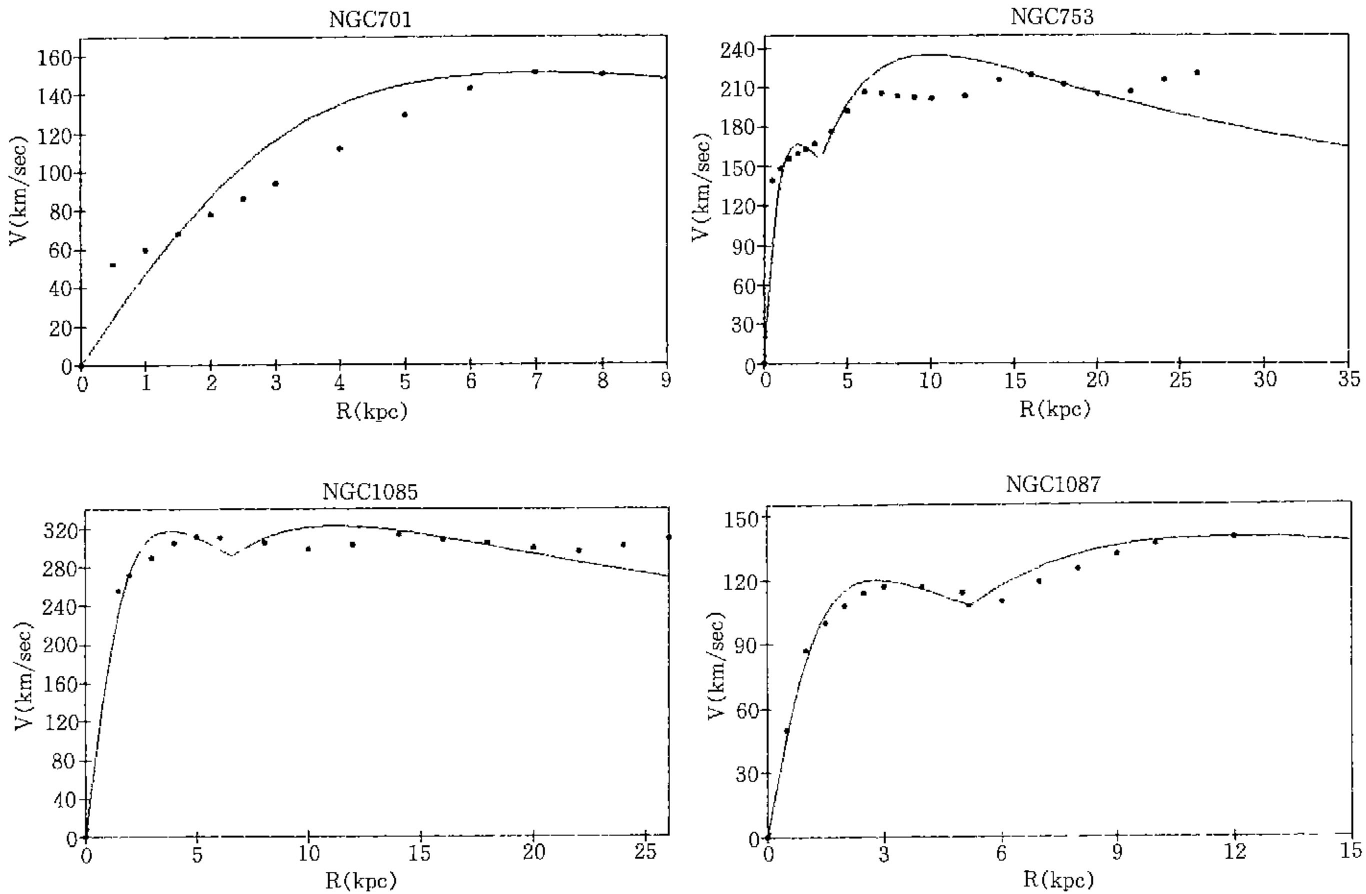

Fig. 2. The observed rotation curves were fitted to the Toomre's mass model. Most of the sampled galaxies were fitted to n=1. However n=2 was supplied to NGC 4378 and NGC 7171.

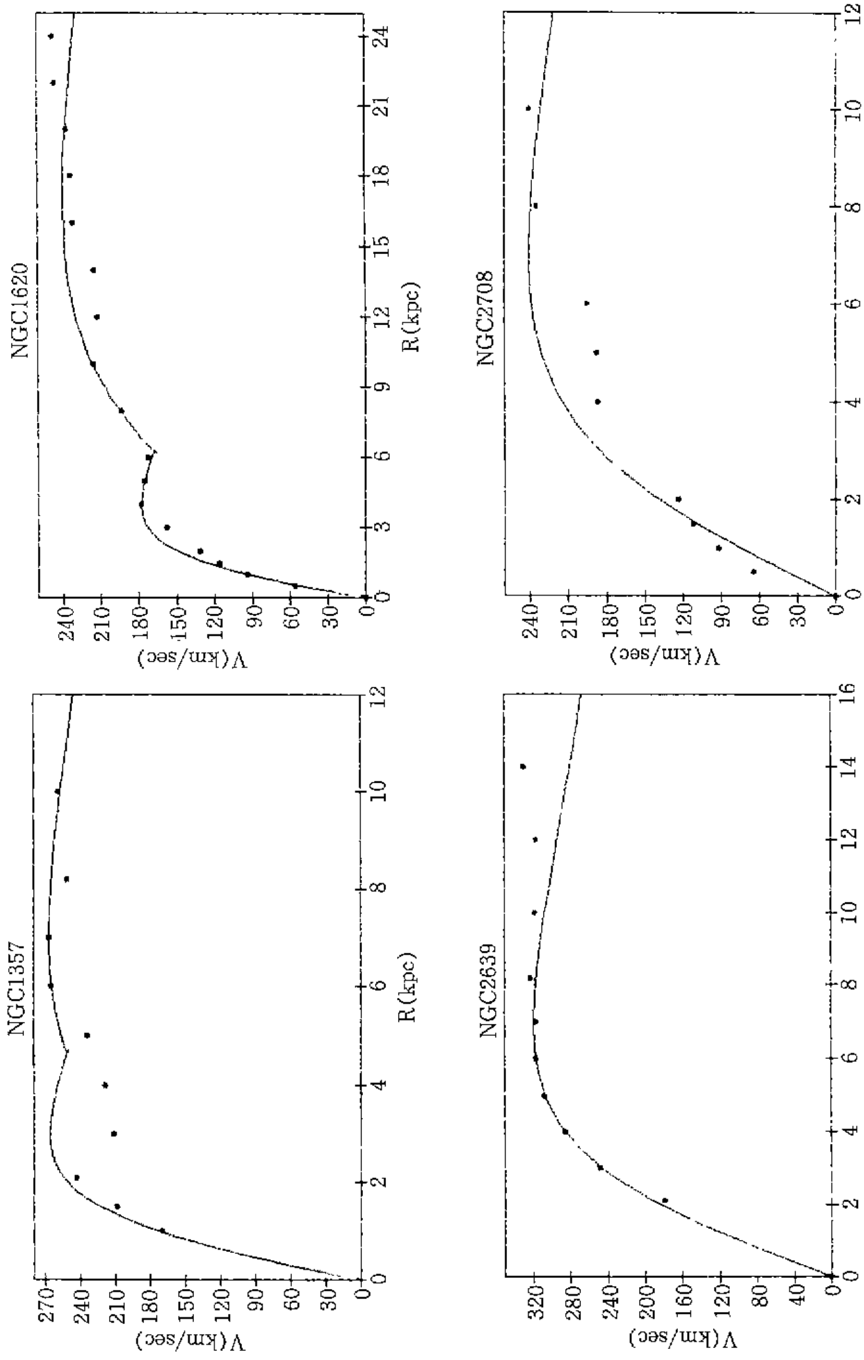

Fig. 2. Continued.

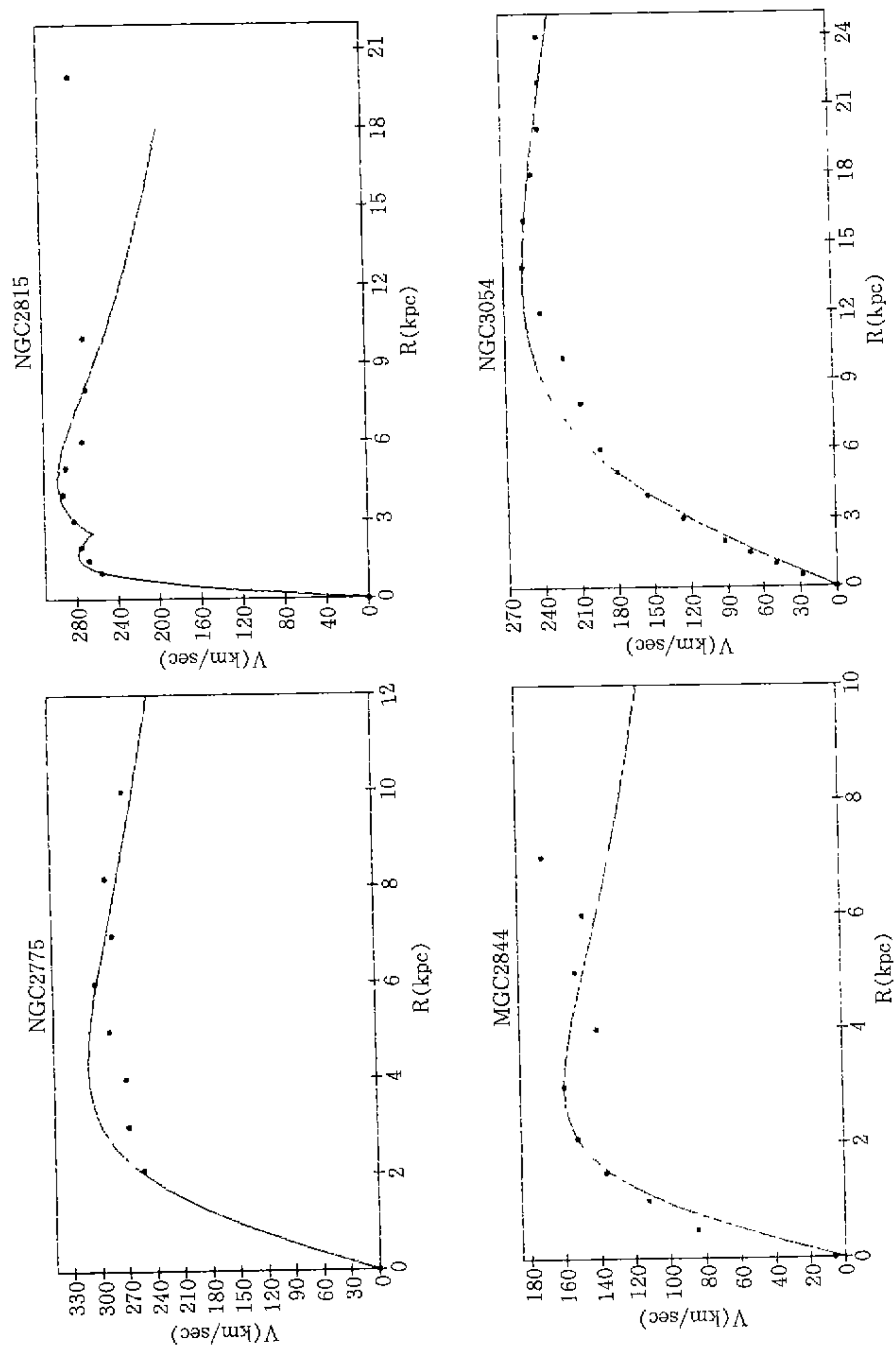

Fig. 2. Continued.

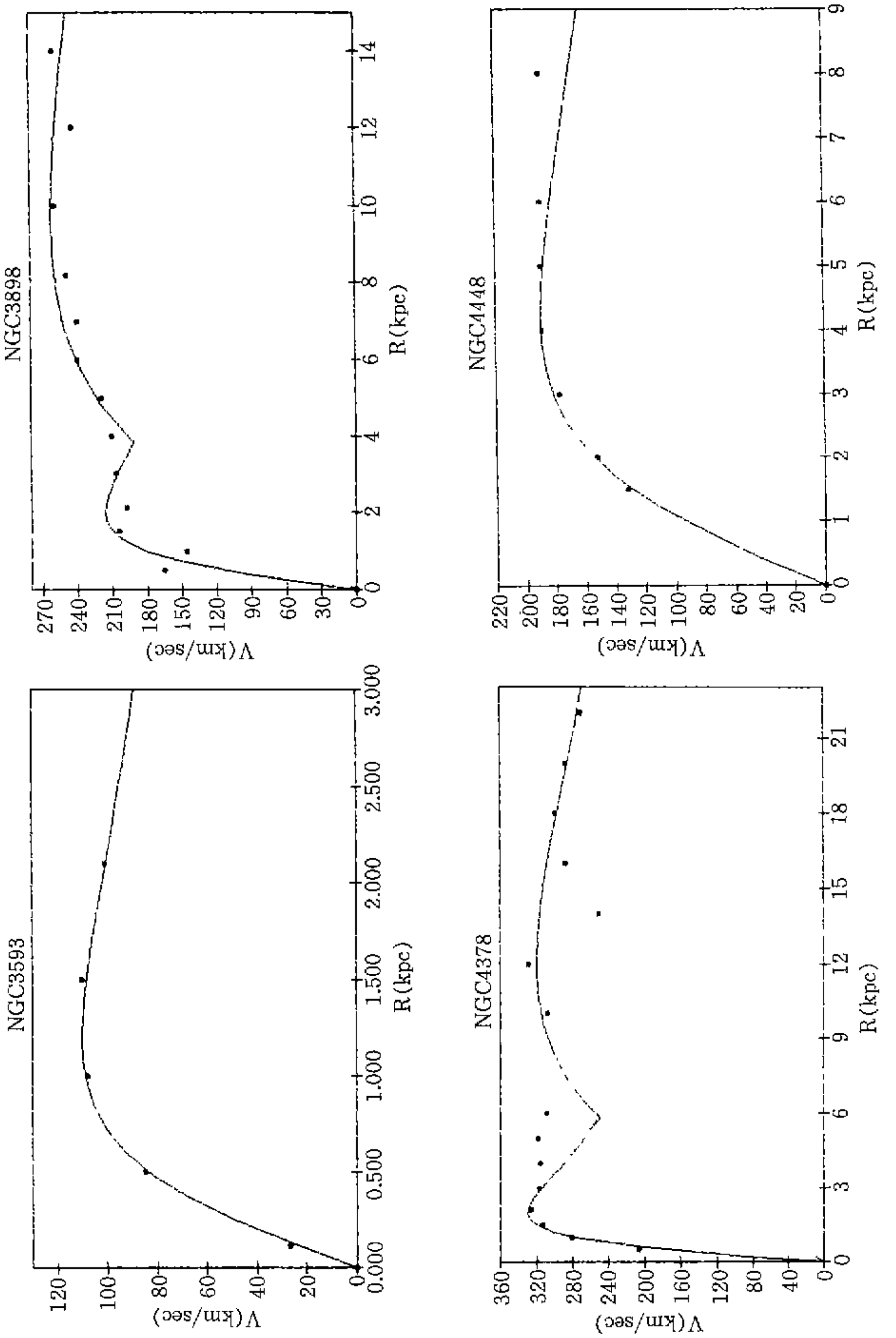

Fig. 2. Continued.

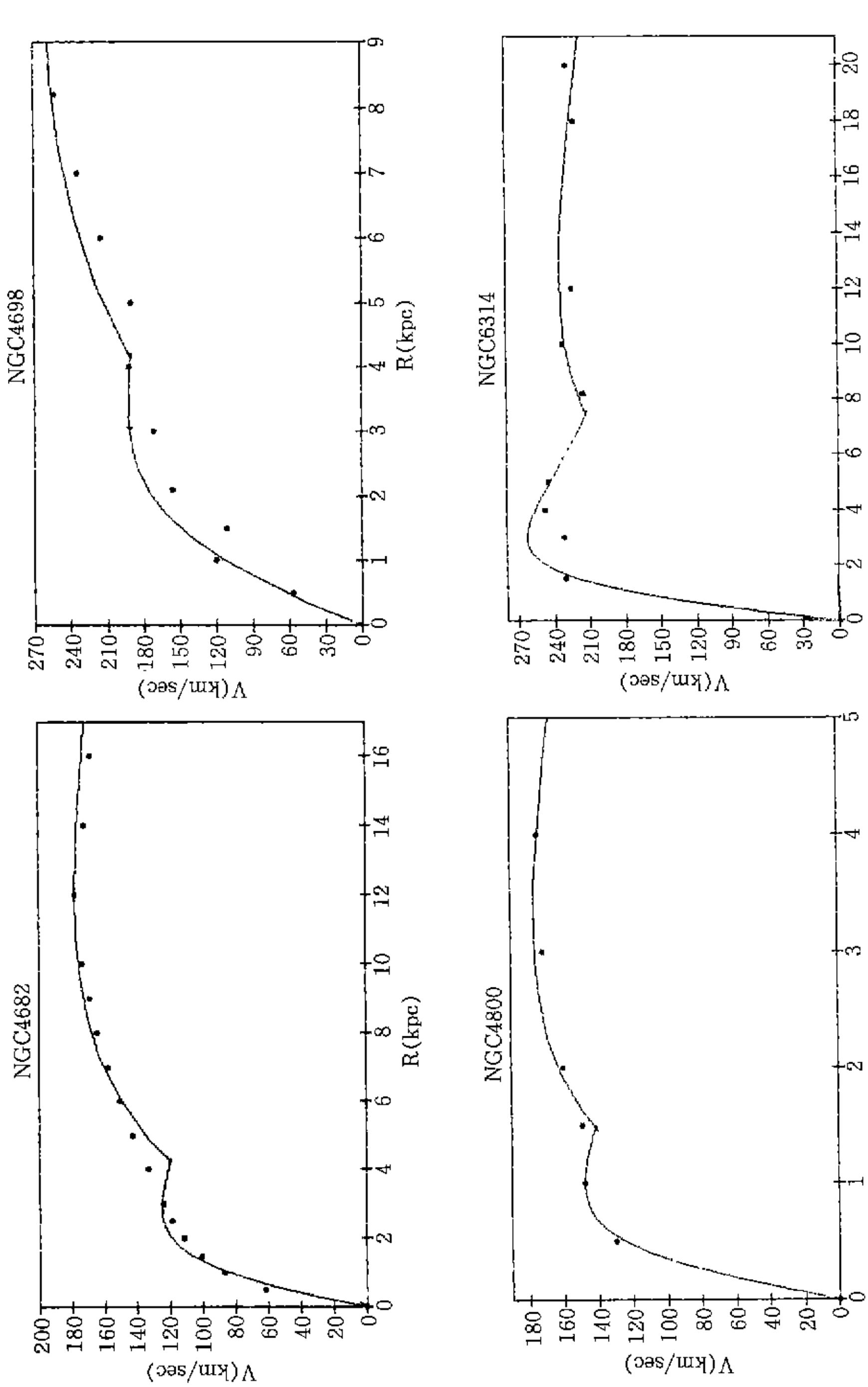

Fig. 2. Continued.

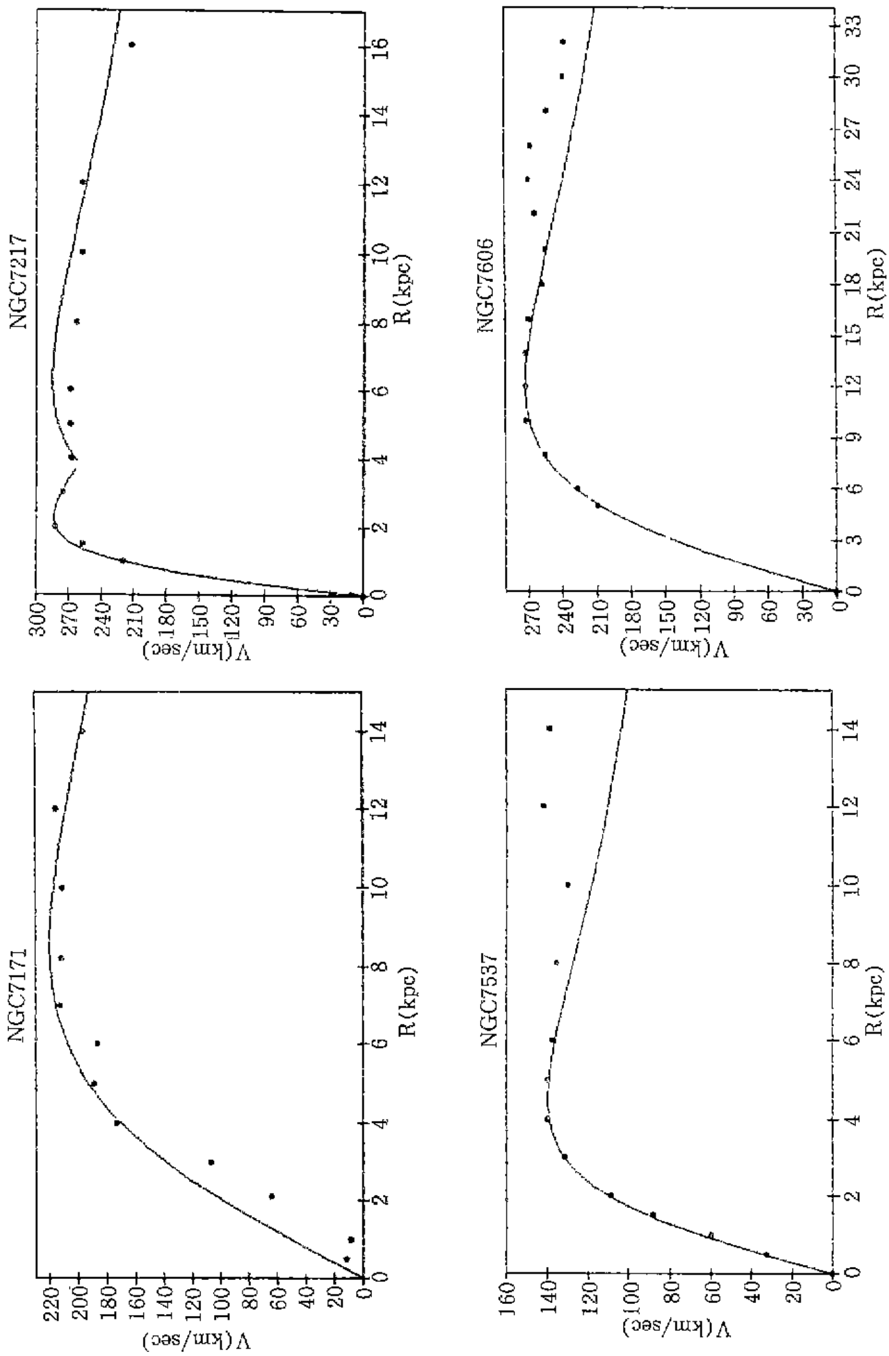

Fig. 2. Continued.

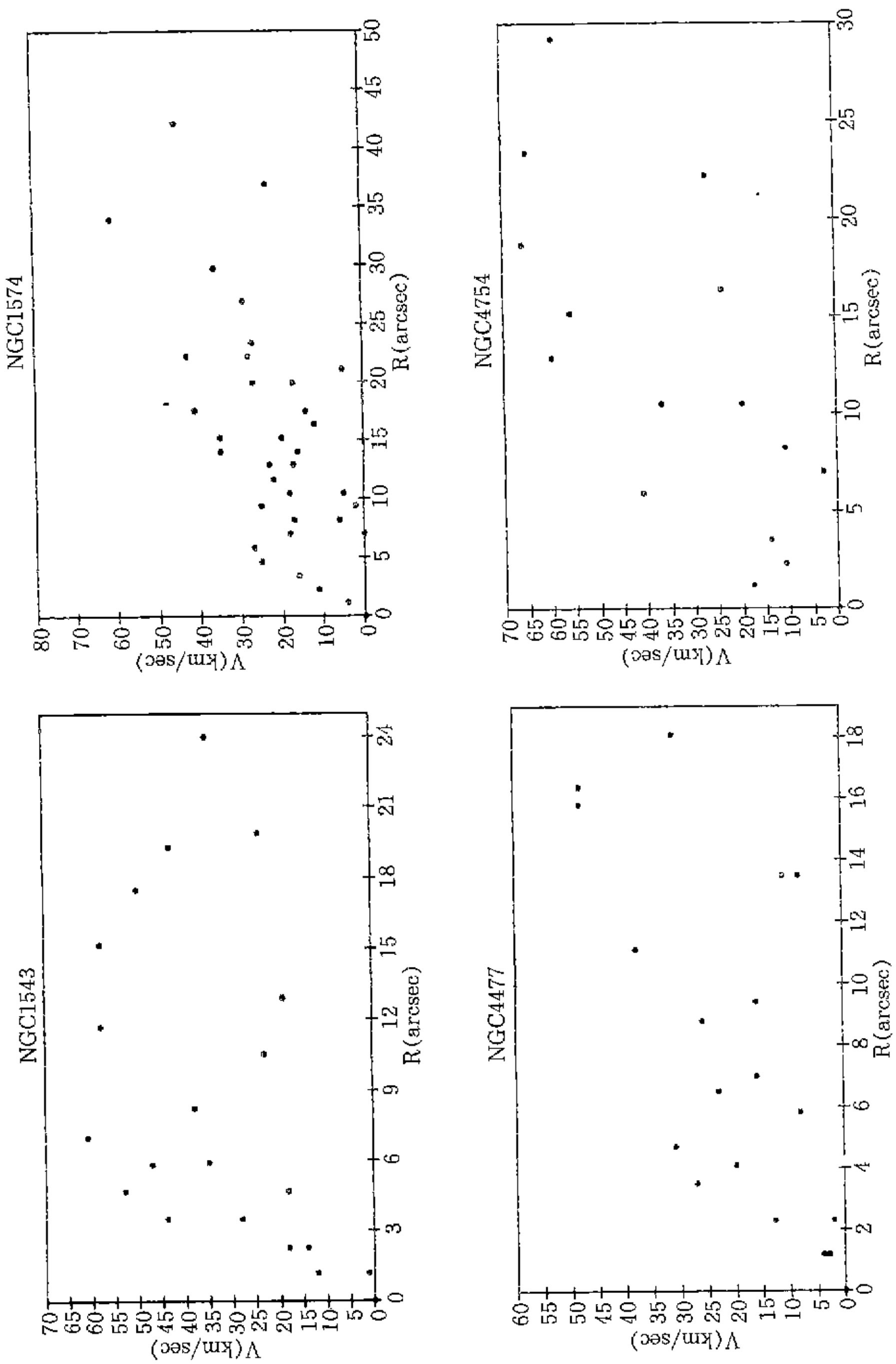

Fig. 2. Continued.

Table 3. Calculated dynamical parameters of 28 galaxies

NAME	Bulge		Disk		M_B	M_D	M_T	$(M/L_B)_T$
	r_{max} (kpc)	V_m (km/sec)	r_{max} (kpc)	V_{max} (km/sec)	($\times 10^{10}$M)	($\times 10^{10}$M)	($\times 10^{10}$M)	($\times 10^{10}$M)
N701			7.0	151			6.8	2.5
N753	2.0	167	9.9	235	1.5	21.4	22.9	1.3
N1085	3.8	318	11.2	323	10.1	38.0	39.0	2.9
N1087	2.8	120	12.0	140	1.1	4.8	5.9	0.8
N1357	3.0	266	7.0	267	0.8	18.8	19.6	2.9
N1543								
N1574								
N1620	4.0	178	17.0	220	3.2	30.5	33.7	2.1
N2639			7.0	320			31.3	3.0
N2708			7.0	241			17.3	4.3
N2775			4.3	312			17.8	2.0
N2815	1.7	278	4.5	297	3.2	12.9	16.1	1.5
N2844			3.0	160			3.3	3.0
N3054			13.5	255			37.4	4.1
N3593			1.2	110			0.6	0.6
N3898	2.0	216	9.7	262	2.6	24.7	27.3	14.0
N4378	2.0	330	12.0	320	7.2	25.0	32.2	2.8
N4448			4.3	190			6.5	2.7
N4477								
N4682	2.9	125	12.0	178	1.1	14.9	16.0	4.4
N4698	3.4	192	10.5	260	2.9	13.9	16.8	2.1
N4754								
N4800	1.0	148	3.3	177	0.1	2.3	2.3	2.8
N6314	3.0	263	12.5	235	6.4	22.4	28.8	1.1
N7171			8.5	220			11.4	2.7
N7217	2.2	283	6.3	285	4.7	9.3	14.0	1.3
N7537			4.5	140			3.8	0.9
N7606			12.0	273			38.1	1.8

V. Discussions

Some physical and dynamical parameters of 28 galaxies can be calculated through the decomposition of luminosity distributions and the model fitting to the rotation velocity curves. From these parameters we tried to find some corelations with structural characters of these 28 galaxies.

a) Disk Component Parameters

i) Correlation between μ_0 and T

We plotted the central surface brightness(μ_0) of 28 extra galaxies to the morphological class (T) in Figure 3. The central dotted line is 21.65mag/arc sec^{-2} which value was suggested by Freeman(1970). However the dispersion is wider than Freeman's suggestion(1970) and tends to be fainter to the early type galaxy. This result is similar to that of Boronson(1981) and Kent (1985).

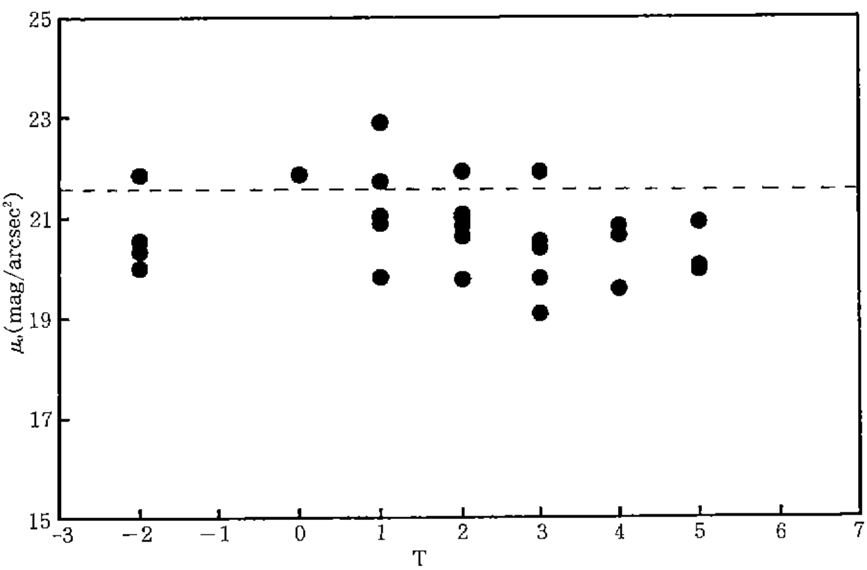

Fig. 3. Correlation between the morphology and the central surface brightnesss of the spheroidal component. The dotted line is the Freeman's value (21.65mag/arc sec). Dispersion is wide.

ii) Correlation between α^{-1} and T

The scale length(α^{-1}) are plotted to the morphological type (T) in Figure 4. The result shows that the scale length is in the range of 1 to 9 Kpc while T=1 to 3. However it becomes 1 to 4 Kpc for the late type galaxies.

This result is quite similar to those of Freeman(1970) and Boronson(1981).

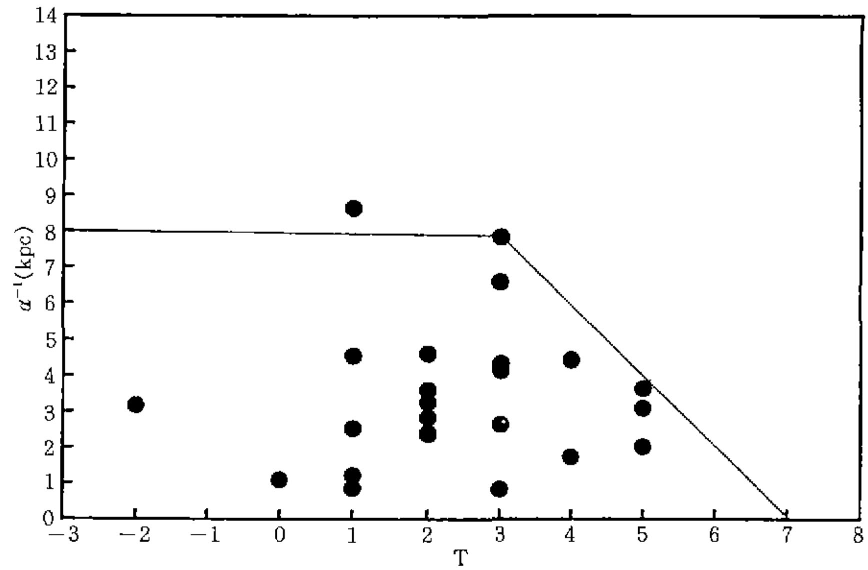

Fig. 4. Correlation between the scale length and the morphology. The dispersion becomes smaller to the late type galaxy than the early one.

iii) Correlation between μ_0 and α^{-1}

In Figure 5 we plotted the central brightness of the disk(μ_0) to the scale length(α^{-1}). From this figure we can see that the smaller the scale length is the brighter the central surface brightness.

b) **Spheroidal Component Parameters**

i) Correlation between μ_0 and T

The central surface brightness of the spheroidal component(μ_e) to the morphology of galaxies is plotted in Figure 6. Unlike the disk component we can see that μ_e becomes fainter from SO to

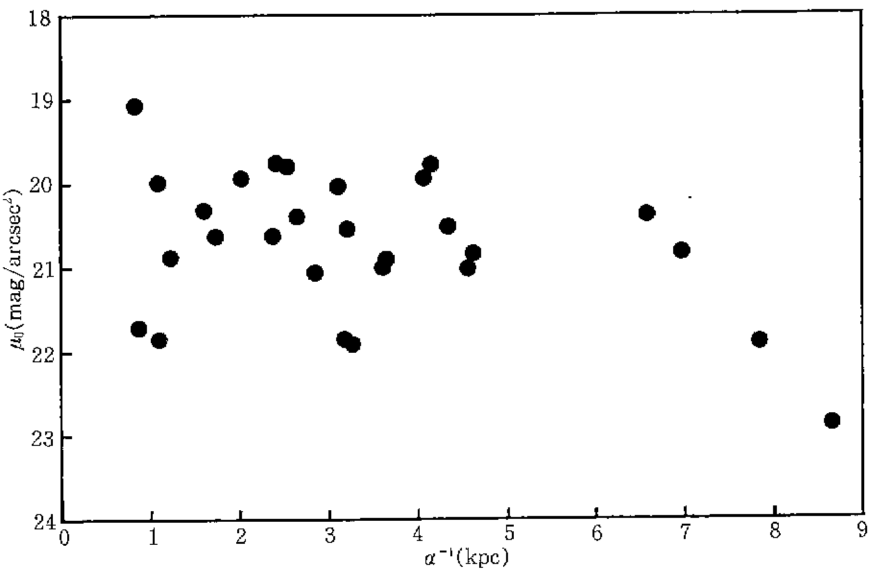

Fig. 5. Correlation between the scale length and the central surface brightness. The central brightnessis fainter to the galaxy with the larger scale length.

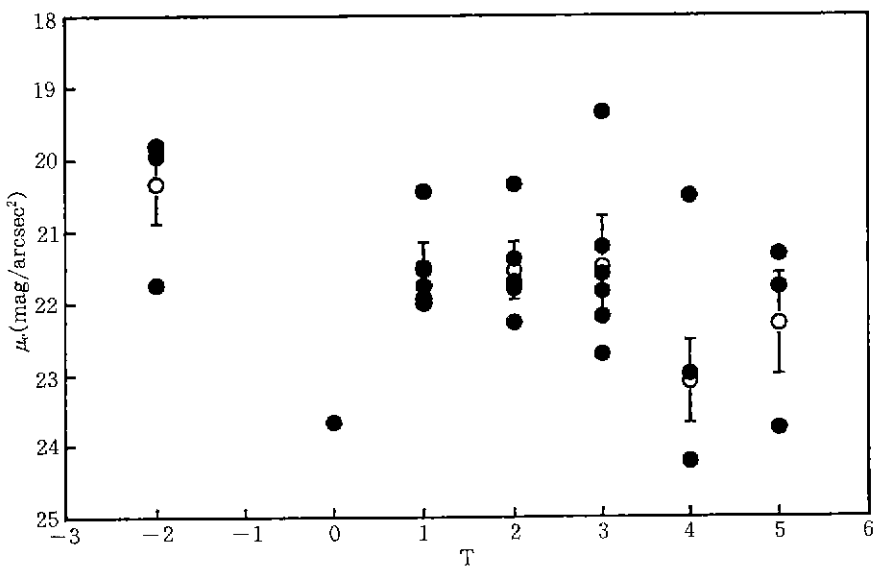

Fig. 6. Correlation between the brightness of the spheroidal component and the morphology. Open circle indicates mean brightness magnitude in each morphologcal class.

Sc by about 2 magnitude. This tendency was found by Kent(1985), Simien and deVaucouleurs (1986).

ii) Correlation between μ_e and r_e

Figure 7 shows the correlation between the central surface brightness of the spheroidal component(μ_e) and the effective radius(r_e). From this figure we can see that galaxies with the smaller effective radius have the brighter central surface of the spheroidal component. However NGC 4682 and NGC 701, both are identified in Figure 7, do not follow this trend. The main reason for this is that these galaxies are the disk galaxy and their D/B values are very high(NGC 4682 is 161 and NGC 701 is 70).

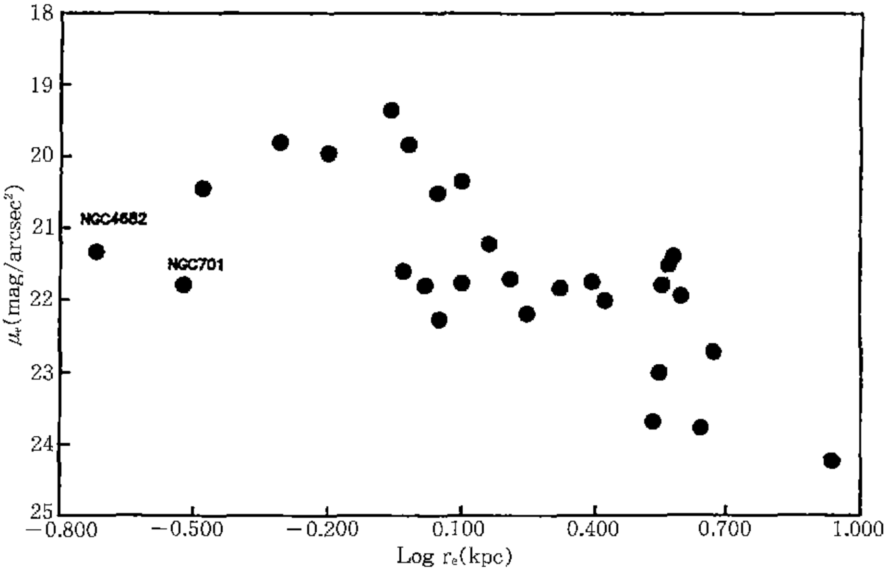

Fig. 7. Correlation between the effective radius and the brightness of the spheroidal component. Galaxies with the fainter spheroidal component have the larger effective radius.

iii) Correlation between D/B and T

The correlation between the disk to bulge ratio (D/B) and the morphological class (T) was studied by Freeman(1970), Yoshizawa and Wakamatsu(1975). In Figure 8 we plotted D/B to T for our studied galaxies. From this figure we can see the marginal increas of D/B value to the late type galaxy. This tendency was confirmed by Kent(1985), Boronson(1981), Simien and deVaucouleurs(1986).

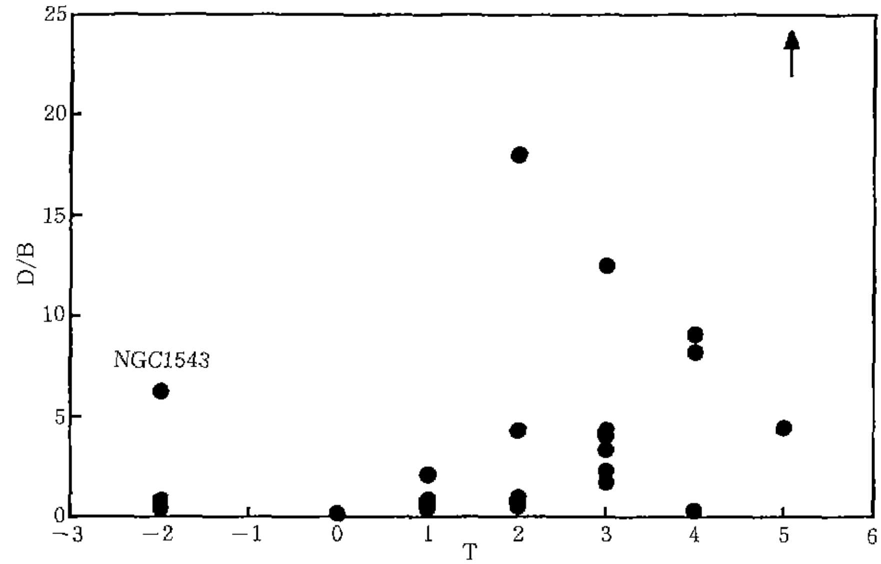

Fig. 8. Correlation between the disk to bulge ratio and the morphology. *Disk to bulge ratio increases in the late type galaxies.*

c) Dynamical Parameters

i) Correlation between M/L_B *and* T

Masses of 24 galaxies were calculated from the fitting of rotation curves to the Toomre's mass model. Rotation curves of 4 SBO galaxies-NGC 1543, NGC 1574, NGC 4754 and NCG 4477-were made only in the central area, we could not fit these curves to the Toomre's mass model.

Maximum rotational velocity of the SO/a galaxy NGC 3593 was estimated as 110km/sec, which is less than 50% of the maximum velocity of the normal Sa galaxy. Because of this low velocity, mass and M/L_B are smaller than those of Sa galaxies. Except these 5 galaxies we plotted mass to luminosity ratios (M/L_B) against the morphology (T) of 23 galaxies in Figure 9. The calculated mass of NGC 3898 from this study is $2.7 \times 10^{11} M_{\odot}$, which is similar to that of Rubin *et al.*(1985).

Figure 9 shows that M/L_B becomes smaller to the late type galaxies, which tendency was found by Faber and Gallagher(1979).

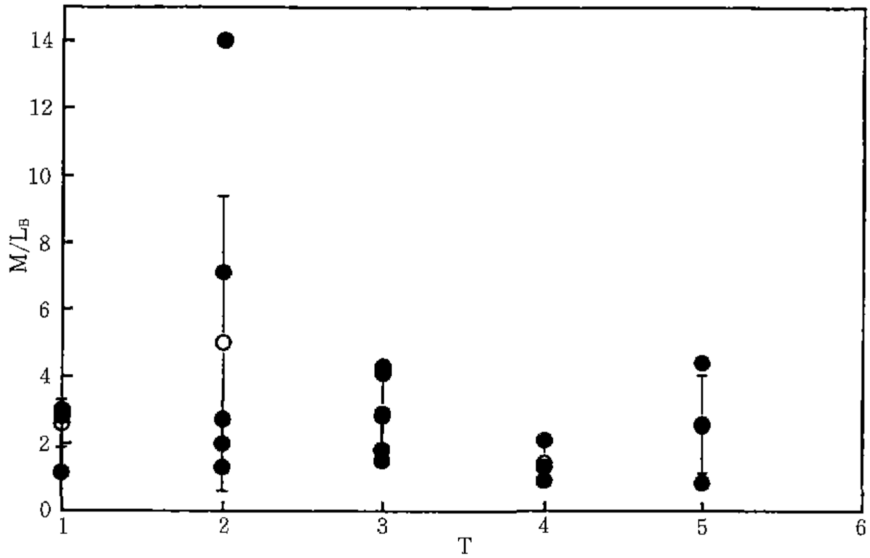

Fig. 9. Correlation between the mass to luminosity ratio and the morphology. The open circle is the mean value of the mass to luminosity ratio in each morphologcal Class.

ii) Correlation between M/L_B and other parameters

In Figure 10 we plotted the mass to luminosity ratio (M/L_B) to the disk to bulge ratio (D/B). From this figure we can see that galaxies with small D/B values have large dispersions of M/L_B values. This phonomenum can be interpreted as the possible existence of dark matter of galaxies with small disk components. Similar correlation was found in Figure 11, which show the relationship between the arm classification (AC) and M/L_B values. Galaxies with well developed arms tend to have small dispersion in M/L_B values.

Figure 12 shows the correlation between the absolute magnitude (M_r) and the mass to luminosity ratio (M/L_B). It seems that the brighter galaxies have the small M/L_B values.

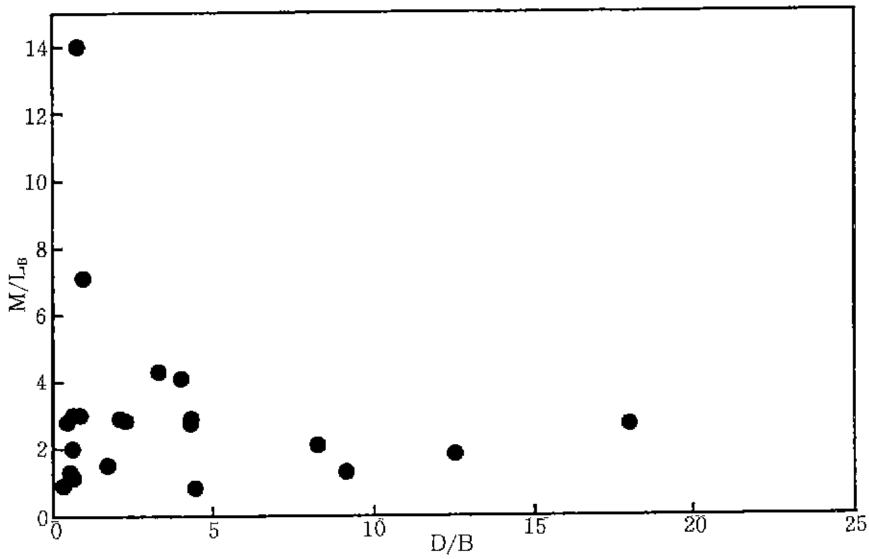

Fig. 10. Correlation between the disk to bulge ratio and the mass to luminosity ratio. Galaxies with large valuses of the disk to bulge ratio have the small and constant mass to luminosity ratio.

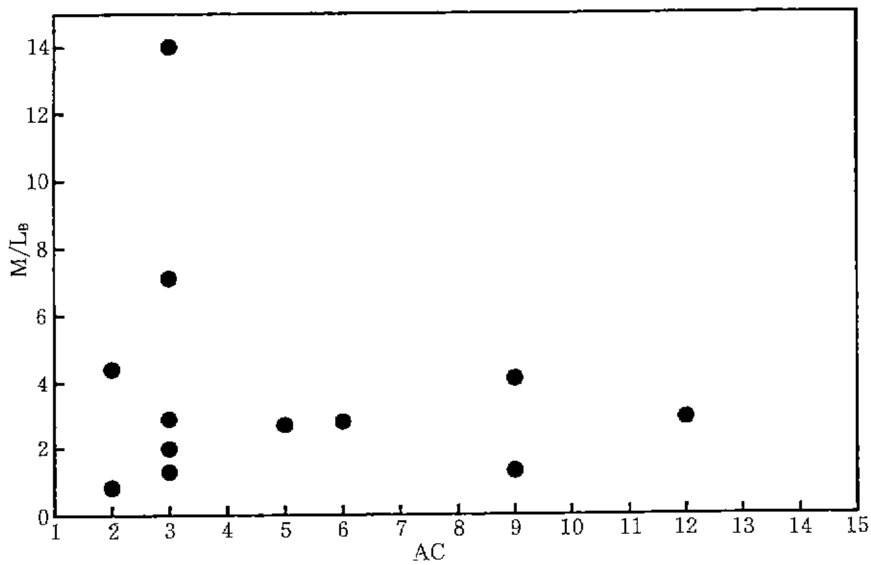

Fig. 11. Correlation between the mass to luminosity ratio and the arm classification. Galaxies with the well developed spiral arms have the small and coustant mass to luminosity ratio.

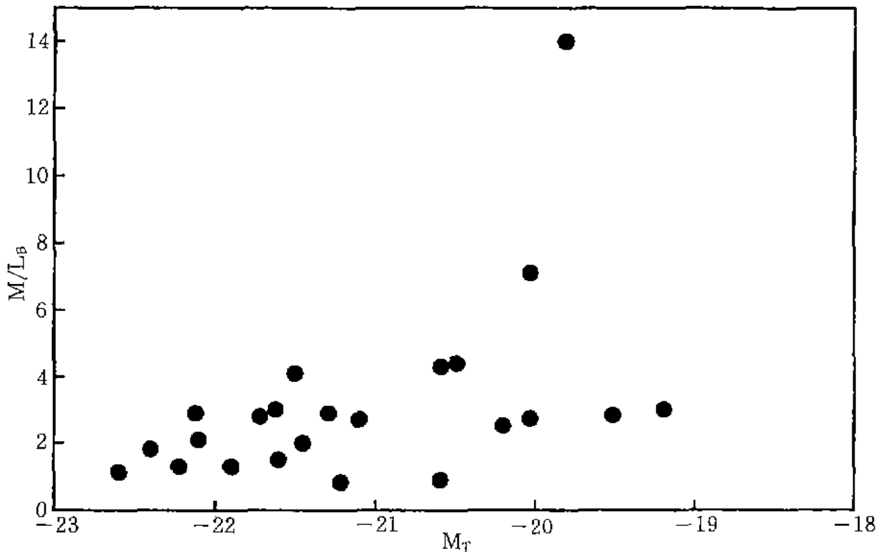

Fig. 12. Correlation between the mass to luminosity ratio and the total magnitude. Marginal increase of the mass to luminosity ratio was found in the fainter galaxies.

Conclusion

From the observed surface brightness distributions and rotation velocities of 28 galaxies we can calculate physical and dynamical parameters of these galaxies. These calculated parameters were compared each other to find possible correlations with the morphology, physical and dynamical characters. The main results we can get from this study are as follow.

1. The central surface brightness of the spheroidal component has wide dispersions, which is contrary to the Freeman's argument(1970).
2. The distribution of the scale length is different between the early and late type galaxies. The galaxy with the fainter central surface brightness of the spheroidal component has a smaller scale length.
3. The brightness of the spheroidal component of the late type has 2 magnitude fainter than the earlier type galaxy.
4. Disk to bulge ratio (D/B) becomes large in late type galaxies.
5. Mass to luminosity ratio (M/L_B) is smaller in late type galaxies.

Acknowledgements

We would like to thank J. H. Park and M. H. Rhee for their help and suggestions in this work. This work was supported by the Yonsei University research grant in 1989.

References

Boronson, T. 1981, *Astrophys. J. Suppl.*, **46**, 177.

Brandt, J. 1960, *Astrophys. J.*, **131**, 293.

Burstein, D. 1979, *Astrophys. J*, **234**, 435.

de Vaucouleurs, G. 1953, *Mon. Not. Roy. Astron. Soc.*,**113**, 134.

de Vaucouleurs, G., de Vaucouleurs A. and Corwin, H. G. 1976, *Second Reference Catalog of Bright Galaxies*(Univ. of Texas:Austin).

Dressler, A. 1980, *Astrophys. J.*, **236**, 351.

Elmergreen, D. M. and Elmergreen, B. G. 1987, *Astrophys. J.*, **314**. 3.

Faber, S. M. and Gallagher, J. S. 1979, *Ann. Rev. Astron. Astrophys.*. **17**. 135.

Freeman, K. C. 1970, *Astrophys. J.*, **160**, 811.

Hubble, E. 1936, *The Realm of the Nebulae*(Yale Univ. Press:New Haven).

Jarvis, B. J., Dubath, P., Martinet, L. and Bacon, R. 1988, *Astron. Astrophys. Suppl.*, **74**, 513.

Kent, S. M. 1984, *Astrophys. J. Suppl.*, **56**, 105.

Kent, S. M. 1985, *Astrophys. J. Suppl.*, **59**, 115.

Kent, S. M. 1986, *Astron. J.*, **91**, 1301.

Kent, S. M. 1988, *Astron. J.*, **96**, 514.

King, I. R. 1978, *Astrophys. J.*, **222**, 1.

Kormendy, J. 1977, *Astrophys. J.*, **217**, 406.

Mestel, L. 1963, *Mon. Not. Roy. Astron. Soc.*,**126**, 553.

Rhee, M. H. 1988, MSc thesis, Yonsei University.

Rubin, V. C., Ford, W. K. Jr. and Thonnard, N. 1980, *Astrophys. J.*, **238**, 471.

Rubin, V. C., Ford, W. K., Jr., Thonnard, N. and Burstein, D. 1982, *Astrophys. J.*, **261**, 439.

Rubin, V. C., Ford, W. K., Jr. and Thonnard, N. 1985, *Astrophys. J.*, **289**, 81.

Sandage, A. 1975, *Galaexies and the Universe, Stars and Stellar Systems* vol. IX, ed. A. Sandage,

M. Sandage and K. Kristian(Univ. of Chicago:Chicago), pp. 1-35.

Sandage, A. and Tammann, G. A. 1981, *A Revised Shapley-Ames Catalog of Bright Galaxies*(Carnegie Institution of Washington:Washington).

Shombert, J. M. and Bothun, G. D. 1987, *Astrophys. J.*, **92**, 60.

Schweizer, F. 1979, *Astrophys. J.*, **233**, 23.

Schweizer, F. 1981, *Astron. J.*, **86**, 662.

Simien, F. and de Vaucouleurs, G. 1986, *Astrophys. J.*, **302**, 564.

Talbolt, R. J., Jensen, E. B. and Dufour, R. J. 1979, *Astrophys. J.*, **229**, 91.

Toomre, A. 1963, *Astrophys. J.*. **138**, 385.

Yoshizawa, M. and Wakamatsu, K. 1975, *Astron. Astrophys.*, **44**, 363.